Acta Astronautica 229 (2025) 113–127

Contents lists available at ScienceDirect

Acta Astronautica

journal homepage: www.elsevier.com/locate/actaastro

FlyRadar – targets for future drone based GPR survey on mars

Akos Kereszturi [a,*], Gian Gabriele Ori [b,c], Nicole Katerin Dias Marques [b], Philippe Grandjean [e], Pascal Allemand [e], Vilmos Steinmann [a], Gianni Alberti [f], Marco Mastrogiuseppe [g,h], Joanna Gurgurewicz [d], Wlodek Kofman [d,i], Daniel Mège [d], Claudio Orlanducci [d], Pierre-Antoine Tesson [d], Osip Kokin [b], Sylvain Augier [e]

[a] Konkoly Astronomical Institute, Research Centre for Astronomy an Earth Sciences, Budapest, Hungary
[b] International Research School of Planetary Sciences, Università d'Annunzio, Pescara, Italy
[c] Ibn Battuta Centre, Marrakech, Morocco
[d] Centrum Badań Kosmicznych Polskiej Akademii Nauk (CBK PAN), Bartycka 18A, 00-716, Warszawa, Poland
[e] Universite Claude Bernard Lyon 1, ENS Lyon, Université Jean Monnet Saint-Étienne & CNRS, Laboratoire de Géologie de Lyon, Terre Planètes Environnement, UMR 5276, 69100, Villeurbanne, France
[f] ATG Italy s.r.l., Via Ludovisi 16, 00187, Roma, Italy
[g] Link Campus University, Via del Casale San Pio V, 44, 00165, Rome, Italy
[h] Sapienza Università di Roma, Via Eudossiana 18, 00184, Italy
[i] Univ. Grenoble Alpes, CNRS, CNES, IPAG, 38000, Grenoble, France

A B S T R A C T

The possibility and feasibility of future drone-based shallow subsurface GPR radar survey for Mars have been examined. SHARAD data indicates shallower features are expected to be present, while HiRISE based analysis of outcrops confirm there are several target features, waiting for radar identification. Targets for an airborne shallow subsurface radar were evaluated including ice content of indurated dunes, internal layering of fluvial deposits, mid- and high latitude ice containing features, former crater lake sediments and lava caves; as well as expected dielectric constant values. The proposed instrument will be able to explore discontinuities in the underground to measure thickness, volume and stratigraphic sequence. Airborne GPR is expected to provide such information what is not achievable by rovers with limited traverse capability and inability of crossing several terrain types.

The radar penetration will be increased compared to those characteristics on the Earth by the low humidity expected in the Martian subsurface, while the iron-oxides could decrease the signal with scattering effect and the normal attenuation due to imaginary part of dielectric constant. As radar signals are strongly affected by the presence of liquid water that is very common of Earth, the FlyRadar instrument will be tested mostly in dry areas that are arid hot deserts, karsts or cold arid areas where water is frozen. The suggested trade off according to the geology of the investigated areas was found for the survey of the top 50 m of subsurface could be done at 20 MHz of bandwidth with 80 MHz of transmitted frequency. The mass of such an instrument could reach kilogram payload. The drone technology is available to do survey at 10 km scale distances, what neither an orbiter nor a surface rover could achieve, in order to support next missions for science and ISRU activities.

1. Introduction

This work presents the needs and the general characteristics of a shallow radar survey deployed on Mars, presenting what type of features could be observed by a shallow subsurface ground penetrating radar (GPR) together with the observation strategy and instrument characteristics. Range of scientific questions on tectonics (shallow deformation, mass movements), volcanism (lava stratigraphy, caves, plumbing system, role of volcano-ice interaction), climate evolution (depositional and desiccation features from recent climate changes in the Amazonian), water and ice (partly identified shallow occurrence) etc. could be answered of partly clarified with better knowledge on the shallow subsurface of Mars [1]. Beyond these general aims, this work is also to outline the need for a specific UAV supported GPR system for Mars, called FlyRadar.

As the presented geological features hold **important information** for Mars research and **in-situ resource utilization** (ISRU) activities, which are expected to be important targets in the next decade. While the top surface is influenced by UV- plus charged particle irradiation, as well as heavily oxidized, the few meters deep region is not influenced by these effected, thus should be target for the acquisition of astrobiology relevant materials. However, it is accessible by shallow drill and

* Corresponding author.
E-mail address: kereszturi.akos@csfk.org (A. Kereszturi).

https://doi.org/10.1016/j.actaastro.2025.01.012
Received 11 June 2024; Received in revised form 8 November 2024; Accepted 6 January 2025
Available online 7 January 2025

excavation. GPR exploration could be a good alternative for ground exploration. While meteorological conditions could desiccate the top few centimeters to decimeters of the regolith, several meter deep layers might hold large water ice masses that have been preserved for millions of years, supporting valuable targets and source raw materials. This several meter deep weakly modified zone holds important information on the Martian past, and can be moderately easily accessible for on-site works, especially by the first manned mission.

1.1. Importance of radar observations

Radar observations are important for Mars and based on the former MARSIS [2–4] and SHARAD instruments used from orbit, the RIMFAX instrument onboard the Perseverance and RoPeR instrument onboard Zhurong rovers could provide a range of such discoveries, which would have not been possible to be achieved by other methods, including remote sensing and on-site techniques. Internal structure of the polar caps [5], thickness so some depositional units [6], occurrence of buried ice masses [7] have already demonstrated the success of GPR-like technology for Mars. The discoveries of shallow subsurface ice on Mars ([8], Morgan et al., 2015, [9,10]), and the mapping of these deposits (Putzing et al., 2023, [11]), which could be used for climate reconstruction and ISRU activities, make shallow subsurface region especially important for GPR studies. However, these targets in the top 1–50 m shallow part of the regolith are situated above the upper mentioned SHARAD ideal survey depth, and the rovers could not provide wide aerial surveys – despite this top several meter parts will be the target of ISRU activities and accessible by drills for the first human mission also, as well as targeted sample return in the future. Thus, this depth range is important, and it is needed to identify how radar based observations could survey and discover features there.

1.2. Earlier radar surveys on mars

Despite these major aspects, the excavations and drills realized until now **did not penetrate below** the top decimeter layer, while sounding radar (occasionally also named as orbital based ground penetrating radars) from orbit, such as SHARAD (20 MHz central frequency) and MARSIS (1.8–5.0 MHz central frequencies, with horizontal resolution is about 10 km while the range resolution is 150 m for MARSIS and 15 m for SHRAD in vacuum) have surveyed layers as deep as several 100 m and up to 4 km, respectively. Two surface missions used similar capability: the Perseverance with the RIMFAX radar onboard (150–1200 MHz, [12]), the RoPeR radar onboard the Zhurong rover (450–2150 MHz, [13]). Perseverance found buried boulders or cavities located in the upper 5 m of the subsurface [14]. The produced subsurface map of Máaz and Séítah formations shows distinct reflector packets of low-radar reflectivity from potential depositional hiatuses inside mafic material. This solid material composition is based on permittivity around 9.0 and bulk density of 3.2 g cm^3 [15]. Measurements have shown a constant-Q around permittivity of 7 is 78.8 ± 11.6, for a subsurface propagation velocity of 0.113 m/ns, what equals an attenuation of −2.1 ± 0.4 dB/m at the RIMFAX 675 MHz center frequency [12]. Results of the Zhurong GPR identified layered subsurface structure at Utopia Planitia with buried polygonal terrain below a depth of 35 m [16]. The observed permittivity of the regolith within 5 m of the landing zone is $3.6^{+3.1}_{-2.0}$, and the average loss tangent is $0.0174^{+0.0053}_{-0.0053}$ [17] with high dispersion of both permittivity and loss tangent values indicating heterogeneous material distribution. Wisdom GPR [18] is expected to work onboard of the Exomars rover. Observations of these two rover missions were useful to partly reconstruct the geological history of the terrain. However, the analysis was limited to a specific distance, and the lack of an aerial survey, with only one stripe profiling, restricted the range of findings that could be drawn from the identified features and regional changes.

Beside the scientific aspects, this work **aims** to provide a comprehensive overview of the technical possibilities of a drone-based GPR method for future implementation. Section 3.1 lists examples of available technology, while Section 3.2 identifies potential targets and discusses measurements already carried out on Mars. The discussion in Section 4 outlines the possibilities and strategies that such a mission should follow, evaluating the knowledge gaps in Section 4.1 and technology needs in Section 4.2. Using the proposed method, such a GPR onboard a Martian drone could survey shallow subsurface water ice masses for climate reconstruction and ISRU activities. Additionally, it could investigate possible occurrence of shallow water or brine, even at the microscopic scale, for astrobiology research and several further geological applications can be envisaged. Such a project could identify and improve knowledge on subsurface layering and various geological features in order to reconstruct geological history. Additionally, it seeks to identify the depth of any interesting subsurface feature, assisting to identify the optimal drilling location for physical access. Drones on Mars with shallow subsurface survey capabilities could ideally support drilling rover missions in the near future, including further Mars Sample Return activities.

The findings of this paper contribute to **paving the way of future** regional subsurface analysis on Mars using drones. The experience used in this research is among others supported by the former test of the radar/altimeter for the Entry, Descent and Landing of ExoMars 2016 and ExoMars 2020 missions conducted in Erfoud, Southern Morocco, managed by Ibn Battuta Center and some authors of this work [19], in collaboration with Thales Alenia Space Italia and the European Space Agency.

1.3. Background of GPR technology to apply for mars

GPR detects reflections of electromagnetic waves when the signal crosses interfaces marked by impedance contrasts (by dielectric permittivity, and the distances measured by the time interval between the emitted pulse and the received echoes. As the **used frequency** increases, attenuation also increases, leading to a decrease in exploration depth. However, these parameters are dependent on the kind of material (although the range of variation among rock compositions is not so wide). Higher frequency provides improved resolution, while lower frequency penetrates deeper. Additionally, an increased electrical conductivity decreases the penetration depth. Based on the earlier radars systems used for Mars, MARSIS and SHARAD achieved spatial resolution on the scale of 50–500 m and maximum penetration depths, whereas WISDOM, on the planned ExoMars rover, will be able to survey the top 3–10 m with a spatial resolution down to few centimeters using the current plan (Hervé et al., 2022). However, it is important to note that the resolution can be further improved in post-processing using dedicated algorithms like noise filtering, interference suppression technique, using diffraction curves etc. as demonstrated in various studies on Sounder data [20,21] and GPR [22]. Currently, the top 10–30 m of the regolith with areal coverage and a resolution down to 0.5–1 m have not been targeted yet.

Fig. 1 shows the typical attenuation due to ohmic loss and scattering losses of GPR. Ohmic attenuation is inversely dependent on conductivity of the medium and the frequency used. Attenuation increases with higher water content, not because pure water is not well conductive, but because water melts salts in the material by increasing its conductivity. If a subsurface water table is present, it will provide a reflection rather than absorption when there is a significant contrast in the dielectric permittivity between the water and the surrounding material [23]. This might occur on Mars both for pure liquid water and brines (Pál 2021). However, the behavior also depends on the resolution and wavelength of the used instrument. The spatial resolution depends on the transmitted bandwidth (B) that is limited to a certain percentage of central frequency (f0) (and also on the wide/narrow of emitted wavelength range), usually one quarter of the maximal wavelength is a rough approach of maximal resolution.

Larger bandwidth, which can be achieved with higher frequencies,

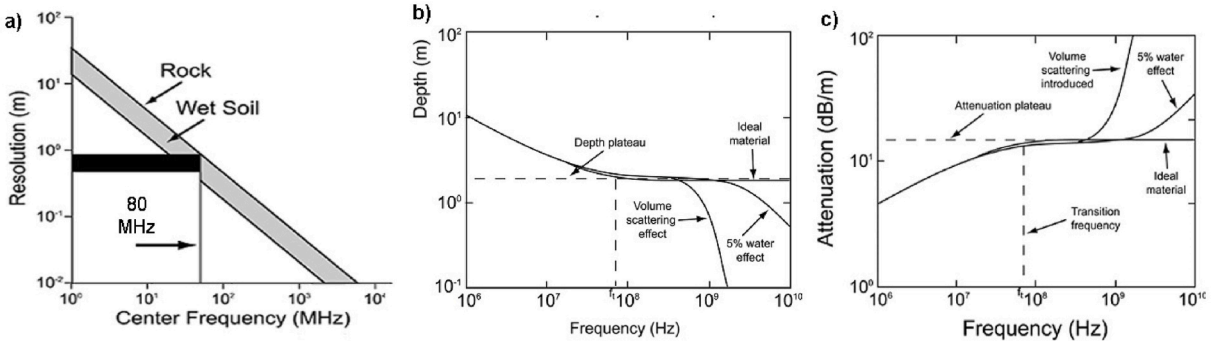

Fig. 1. Left: spatial resolution versus frequency for hypothetical wet and dry targets. The planned about 80 MHz system (see later) allows the spatial resolution in theory around 1 m. Middle: Decrease of exploration depth with variance of frequency. Right: Connection between attenuation (vertical axis) and frequency, which influence exploration depth. In a hypothetical ideal material the attenuation follows a plateau above the transition frequency (dashed lines). However, in real environments water and volume scattering cause increasing attenuation with frequency (source: https://www.sensoft.ca/range-of-gpr/).

allows for better resolution, enabling the identification of smaller details. The resolution is determined by the transmitted bandwidth (B), where time resolution is $\frac{1}{B}$. Spatial resolution can be expressed by the $\frac{1}{2}\frac{v}{B}$ relation, where v represents the propagation velocity (in material less than light speed). However, the greater is the ratio of $\frac{B}{f}$ (f central frequency), the more challenging it becomes to develop the radar system (Fig. 1).

A further important GPR based value is the loss tangent (also known as the "loss factor"), what is a measure of the efficiency of how a particular material converts the electromagnetic energy at different frequences and temperatures. The loss tangent represents the ratio of the imaginary and the real parts of the dielectric permittivity (Campbell & Morgan, 2018).

1.4. Permittivity values of mars relevant materials

The permittivity of materials generally varies with frequency, temperature and humidity. On Mars, it is expected that the shallow subsurface consists mainly in porous basaltic materials together with various salts, especially sulfates and iron-oxides, as well as ice. The potential target materials and their general characteristics are listed in Table 1. It is less probable but might be very important both for scientific research and ISRU activities that brines and humidity might be also present in the subsurface. The porous voids if filled by brine or ice could increase electrical conductivity and cause strong radar reflection [24].

Detailed laboratory analysis was conducted on the permittivity of $CaCl_2$ solutions, which heavily depends on temperature. Below −53 Celsius, the relative permittivity ranges from 3 to 6, but it increases with temperature and concentration of the solution. Similar behavior is observed for magnesium perchlorates with increasing permittivity above −64 Celsius, while $Ca(ClO_4)_2$ shows an increase between −85 and −78 Celsius, also depending on the concentration. Brine mixtures in JSC Mars-1 regolith simulants also show a range of permittivity values depending on temperature and concentration [32].

Based on the data available for Mars, the mineral composition is moderately well known, and some data is also available on the porosity, which exhibits an elevated value at shallow depths in the regolith, especially inside dunes. Using measurements from the InSight mission pores are expected to be closed around 9 km depth [33], and close to the surface the porosity might be up to about 50–60 % (Grott et al., 2022). Some Earth based laboratory tests analyzed the role of porosity in Mars and Moon simulants regarding permittivity [32]. In possible future surveys, changes in the estimated dielectric constant and porosity would support the separation of different subsurface units both in mineral composition and structural properties at different spatial locations.

1.5. Former GPR field tests at cold terrains on earth

There is a wide literature about using GPR surveys to understand various geological aspects on Earth, including at icy terrains [34]. For comparative discussion of these methods see Schennen et al. [35], Guo et al. [36], and Healy et al. [37]. There is also a wide range of works showing how Earth based results could be applied to Mars (Table 2).

The following specific aspects provide further information to understand the significance of the results listed in Table 2.

- [(a1)]The deepest penetration in the Mars analogue Dry Valleys was about 40 m. Weak contrasts in ε (relative permittivity) and interface roughness may have limited the depth, while the lack of apparent penetration may be more a result of the lack of continuous interfaces in the reworked silt.
- [(a2)]The penetration of 70–80 m in the Fairbanks (Alaska) area was possible because of the lack of silts or clays, which precludes the presence of any significant unfrozen water. Silts and clays, frozen or not, afford little penetration to GPR signals.
- [(b)]The maximum prospected depth is 21 m. The low-frequency "ringing" noise obscured some of the ice base returns, possibly caused by the presence of ash layers.
- [(c)]Up-glacier reflectors intersect the surface near subtle ridges at up-glacier dips of 25–30°. These reflectors are interpreted as englacial debris bands (with thicknesses <1 m) bounding ice units. Subsurface radar velocities of 0.15–0.17 m/ns were consistent with a composition of relatively pure ice.
- [(d)]Galena Creek is a debris covered ice core that was identified as being 20–25 m thick with nested spoons architecture. Sulphur Creek: (1) Localized ice deposits <10 m thick at the stagnant ice mid-section can be found with estimated ice content >77 %. (2) The lower rock glacier was measured at ~30 m thickness, with estimated ice content of ~26–50 %. At Sulphur Creek the ice deposits are significantly thinner, more localized, and buried by surface debris up to 4–5 times thinner than the surface debris at Galena Creek.
- [(e1)]Sulphur Creek Rock Glacier provided thin debris cover that was excavated 90 cm before reaching glacial ice. A notable characteristic of the excavated section was the presence of meltwater and a layer of ice-cemented debris between the graded debris and the glacial ice.
- [(e2)]The presence of liquid water in the active layer may be required to create the sharp dielectric contrast observed at the terrestrial sites. Therefore, with the present-day conditions on Mars, we would not expect to see a strong near-surface reflection, but rather a dielectric gradient. If strong near-surface reflectors are observed on Mars in future missions, this could serve as an indicator that liquid water may have played a role in Martian landscape evolution within the time scale of the extant glaciers.

Table 1
Dielectric relative permittivity of materials anticipated to be found in the shallow Martian subsurface at a frequency around 450 MHz (what differs from the 80 MHz proposed in this work) * mark that basalt shows a wide range of permittivity u to about 40, however the lower range is more abundant [25–27]

Material	Dielectric permittivity at 450 MHz	Dielectric permittivity at 35 MHz	Presence on Mars
Air	1	1	Might be decreased relatively to Earth-measured values because of the about 100 times smaller gas density on Mars
Granite	4–6	5	Not expected on Mars in large volume because of the lack of global plate tectonism most of the planetary history, however some indications exist there might be granite in limited extent on Mars [28–30]
Pumice	2–3	2–3	Present with different porosity, the expected weak weathering on Mars to enlarge porosity, while the dryness in general decreases porosity during eruption on Mars (except very early volcanics), e.g. poorly known
Basalt	3–4.5	6–8	One of the main target materials, which shows a wide range of values *
Basalt vesicular	5.0	5–6	One of the main target materials, which shows a wide range of values *
Dry clay		5–40	Phyllosilicates observed spectrally at old terrains, clay sized grains observed by Curiosity in the mudstone of Gale crater [31]
Dry silt	3–30	3–30	Exists on Mars, mainly in the regolith and buried sediments
Dry sand	3–5	3–5	Exists on Mars, mainly in the regolith and buried sediments
Permafrost	4–5	4–5	Exists on Mars, mainly in the mid- and high latitude regions as a mixture of ice + soil
Wet clay/ wet sand	16–32	16–32	Probably rare in wet state on Mars
Dry sandstone	2–3	2–3	Exists on Mars
Wet sandstone	5–10	5–10	Probably rare in wet state on Mars
Water ice	3–5	3–5	At low latitude under dust/ rock cover
Snow	8–12	8–12	Ephemerally present, but mainly under thin dust/ rock coverage
Liquid water	81	82	Very rare, only in microscopic scale or in salty solution (brine)

Comparing GPR surveys conducted in icy terrains on Earth, the frequency range used, typically falls between 50 MHz and 2 GHz, most often around 100–200 MHz. The observations revealed the presence of ice, typically accompanied by the occurrence of various embedded rocky grain layers. Occasionally, the occurrence of a small amount of liquid water were also detected, however at many cases no liquid phase was identified. The liquid phase can be considered one of the most easily observable radar features. Based on the case studies, it has been

Table 2
Summary of characteristic GPR survey on Earth targeting icy terrains.

Target name, type	Used GPR, frequency	Observed ice characteristics	Observed liquid water characteristics	Reference
Permafrost in Alaska and Dry Valleys of Antarctica	50-100 - 400 MHz	Stratigraphy of permafrost. -Dry Valleys: Stratified silts, sands and gravels of low or little ice content, virtually no water. Glacio-fluvial or glacio-lacustrine origin[(a1)] -Alaska: Frozen sands with possible presence of water probably even within the body of the permafrost[(a2)]	Water table at depths of 20–35 m produced strong reflections (Alaska), where attenuation could give important information on target material. Wet sediments may reflect high rates of attenuation in the signal. The contrast in dielectric properties between frozen and unfrozen water undoubtedly causes the stronger diffractions and reflections.	Arcone et al. (2002)
Permanent ice cap on the summit of a stratovolcano (Jamapa Glacier; Mexico)	400 MHz (static point surveying technique)	Ice thickness (ice base/ bedrock) along profiles[(b)]	No liquid water phases were interpreted.	Brown et al. (2005)
Galena Creek Rock Glacier (Wyoming)	100 MHz	Stratigraphy of debris-bounded ice units (nested spoons type)[(c)]	No liquid water phases were interpreted.	Petersen et al. (2017)
Galena Creek Rock Glacier; Sulphur Creek glacial system (Wyoming)	100 MHz (Sulphur Creek); 50 MHz (Galena Creek)	Internal structure, thickness and purity of the ice[(d)]	No liquid water phases were interpreted.	Petersen et al. (2020)
Ice-cemented/ ice-cored rock glaciers (Gilpin Peak, Colorado; Galena & Sulphur Creek, Wyoming; Sourdough, Alaska)	200 MHz	Glacier geometry and structure. Debris mean thickness measured from GPR (for all of the sites): 2 m[(e1)]	A film of meltwater at the debris-ice contact was observed in most of the shallow debris measurement sites[(e2)]	Meng et al. (2020)
Permafrost tunnel (Fairbanks, Alaska)	1–2 GHz (GPR constant offset profiles)	Ice-frozen loess detection (seismic data) displaying relatively large Q values (~80; indicative of low seismic attenuation).	Water-ice content tends to decrease with depth below the floor of Permafrost Tunnel. Overall, large variations were inferred.	Lorenzo et al. (2022)

observed that elevated electrical conductivity causes loss of signal strength. However, it is expected that the moisture content on Mars is lower. phenomena, along with conductive areas that absorb microwaves. These factors should be also considered during the planning of a Martian survey as might be important for the regolith.

Experiences from two **orbiting GPR instruments** are available for Mars. The first instrument is MARSIS radar on-board ESA's Mars Express spacecraft, which was designed to investigate the Martian ionosphere and the geological and hydrological structure of the subsurface, with a particular emphasis on the detection of deep bodies of solid or liquid water.

Considering former drone-based activities, the Ingenuity helicopter successfully demonstrated how is it possible to fly on Mars despite the low atmospheric density (Balaram et al., 2021), and next missions both for Mars [38] and Titan as the Dragonfly will exploit further drone based research works. Considering Earth based tests, robotic helicopter and rover joint architecture operations were teste in Iceland but without radar [39]. However, a drone based GPR survey was realized, at Sourdough, Alaska, and Galena Creek, Wyoming [40]. On the MALA Geodrone a GPR system was mounted using DJI Matrice 600 Pro. UgCS SkyHub terrain-following system with an altimeter and a distance sensor for obstacle avoidance and maintenance of a constant speed and altitude. Low altitude flight only at 2–3 m above the ground was realized to maximize the SNR, using flight speed between 0.5 and 1 m/s. The survey could resolve the debris/ice interface, debris thickness and to resolve englacial debris bands.

1.6. The need for further radar surveys on mars

There is a knowledge gap regarding the very shallow subsurface of Mars, as SHARAD and especially MARSIS produced data of deeper units. Such meter – decimeter scale spatial resolution data is challenging and could not be gained from orbit, but close to the surface. However, the mobility of rovers is limited, and their scanning capabilities are limited to thin lines over a moderate distance. In contrast, a drone-based GPR survey has the potential to overcome these limitations. It can cover larger areas and provide more flexibility in data collection. This paper outlines the feasibility and expected target characteristics on Mars of a drone base GPR survey, partly including the technical capability and needs for the instrument, however the detailed presentation of technical aspects are beyond the scope of this paper.

2. Methods

In this study, we have combined a literature overview of Martian features and physical background of GPR technology. The new aspects and findings presented in this work are the target evaluation and prediction of observable characteristics, along with ranking of various targets and strategies in order to plan drone based GPR analysis for future Mars missions. The possible targets were analyzed using high resolution HiRISE [41] optical images, recorded by the MRO mission from Martian orbit.

During the discussion of technical possibilities, the current knowledge provided the background, however development in the future could increase possibilities and modify the findings of this work. The general aspects and physical laws of GPR signal behavior are only occasionally cited, but further information could be found in Daniel [42].

3. Results

This section provides examples of findings from previous GPR measurements using SHARAD observations, which primarily targeted larger and deeper subsurface structures than can be targeted from a drone on Mars. Then the smaller and shallower subsurface structures are characterized using HiRISE images, which will be the targets for a drone-based survey. After collecting and characterizing the expected targets, the related technological aspects are presented, which should be fulfilled by the future missions. Based on these findings, the discussion section will outline the optimal approach to realize such a mission and acquire scientific results.

3.1. Example targets based on HiRISE images

Surveying about 100 HiRISE images, the examples show the existence of subsurface structures expected to be observable in the top 10–20 m using the proposed radar technology. In Table 3 some examples are listed for the observed structures in the shallow subsurface, exposed by erosion and/or at slopes. These features are usually too small to be resolved by SHARAD, however could be widespread on Mars, and their indications can be found often as exposed layer heads in HiRISE images (Fig. 2).

A potential critical but unknown aspect is the permittivity contrast between various subsurface layers observable in Fig. 1. Based on theoretical considerations, a large compositional difference is not expected often but still could be present in certain cases, like buried observed snow [43] or ice (Harish et al., 2020), dune material [44] layers on Mars. However structural differences could contribute more often to permittivity contrast production. Subsequent ejecta layers might emerge as porosity with contrast between different layers as porosity decreases inside each separate ejecta layer (partly similar was identified by GPR of Chang-E′3 on the Moon, [45]), while buried atmospheric dust layers, former surface exposed sulfate plus hematite cemented duricrust formation [46] also produce density and porosity contrast. Examples from the Earth indicate even basalt lava layers on the top of each other without substantial alteration might results in permittivity contrast. GPR surveyed volcanic terrains on Earth and partly analogous to the Martian surface contain multiple layers of laterally discontinuous fractured deposits that often induce significant scattering loss [47] and their heterogeneities might indicate different layers. Separation of different lava flows was also possible at Craters of the Moon (Idaho, USA) volcanic field [48] using 16–100 MHz ranges.

Based on the items listed in Table 3 the following targets are relevant for shallow radar survey on Mars: there is abundant layering, mainly from recently deposited ice-dust sediments, however there are older structures also. Dunes and dust cover at many locations are present at the surface, however these do not provide strong reflection based on SHARAD observations. If it is possible to establish a connection between subsurface layers that are several meters thick and surface exposures or stratigraphic levels, it would provide a valuable opportunity for reconstructing the geological history of Mars. This level/depth is also important for future manned missions and local ISRU activity there.

3.2. Technology aspects

Calculating with the currently used GPR technology, when aiming the top 1–40 m of the Martian regolith one should use the wavelength range about 100–200 MHz, considering that the penetration is the square root of the frequency as a rule of thumb. The spatial resolution is expected to be in the range of meters or tens of meters horizontally what is controlled by the pulse frequency and UAV velocity. We can expect a horizontal resolution of tHz order of the decimeter, also influenced by the flying altitude of the drone, accuracy of flight trajectory, plus antenna lobe structure, while the vertical resolution heavily depends on the used wavelength. Based on the currently available technology, an instrument around several kg mass and energy consumption around 30 W, and the expected data rate to produce is around 50 Mbytes/s.

Beyond the importance of the scientific aspects, the use of GPR could support future missions with the following aspects: mainly to obtain information on the geometry at depth, to obtain information on surface micro-roughness at the scale of the wavelengths (impossible to obtain by classical photometric techniques), provide information on geotechnical properties of the regolith, better understand ISRU possibilities in

Table 3
Parameters of the HiRISE images indicated in Fig. 2.

Type	HiRISE image no.	Coordinates	Characteristics	Panel no
Crater filling lava or sediments	ESP_069970_1745	5.45S 67.53E	Roughly 1 Ga aged crater filling material (lava or sediment) with exposed subsurface layering by a smaller impact crater along an about 380 m high slope, probably of sedimentary or lava flow layering origin	a
Mantling layer	ESP_069969_2190	38.53N 88.61E	Recent, some Ma old dust + ice deposition with climatic signatures, layer thickness based on shadow length around 6–12 m	b
Scalloped terrains	ESP_069956_2240	43.74N 83.20E	Utopia Planitia cryokarstic terrains, eroded recently deposited volatiles layers of about 2–4 m deep	c
Subsurface voids	ESP_069948_2075	27.44N 302.85E	Collapsed subsurface voids, which might emerge as lack of radar echoes, however in theory at many locations might be ice filled on Mars	d
Layered deposits on valley floor	ESP_069947_1520	27.95S 337.84E	Section of a fluvial valley with 20–25 m thin surface layer cover, possibly formed as earlier fluvial activity or more probable younger sedimentary unit	e
Layering in Western Arabia Terra	ESP_069933_1900	9.69N 355.34E	Erosion exposed shallow subsurface layering in Western Arabia Terra, several quasi-parallel layers are present with about meter thickness	f
Dune covered terrains	ESP_069896_1735	6.54S 287.46E	Bottom level of Candor Chasma probably covered by ancient sediments, but recently became covered by dunes with 1–10 m thickness, with some exposed locations	g

general, especially to provide information on ice occurrence and scientific targets.

4. Discussion

In this section we discuss the expected characteristics of GPR signals on Mars, the potential usage and performance of the technology, and the knowledge gaps that could be addressed by the findings presented in this study.

One important aspect related to the state of subsurface units on Mars is the composition. It is expected that beneath a shallow (decimeters to meters thick) loose **regolith layer** on Mars which contains duricrust and hydration-related mineral filled voids, the deeper regolith might consist primarily of air-filled voids (uncemented grains) in its top layers [49]. However, air filled pores are expected to be mainly present in the upper regions. Using SHARAD (and especially MARSIS) data the identification of such small-scale vertical features becomes challenging. However, sand dunes can be observed in the SHARAD radargrams [50], appearing as weak backscatter signal producing thin features at the surface. In areas where no dune coverage was present, a stronger radar signal emerged directly at the surface, probably due to the abundant scattering sources and the moderate roughness.

The proposed FlyRadar instrument could be used to analyze the vertical and horizontal change in empty/filled voids, facilitating the reconstruction of earlier existing surface layers. This is particularly useful when the regolith was previously exposed and exhibited elevated radar scattering, especially if the geological context is known. Earth based field studies showed that goethite iron-oxide lowers the electromagnetic wave velocity, however neither electrical conductivity nor relative permittivity were altered significantly by iron-oxides, but bound water content has an effect here. As a result, iron-oxides' water content can have an influence on GPR signals with controlling permittivity [51]. The magnetic properties of iron oxides have not been properly accounted for and recent works on Earth based corrosion studies related to GPR signal propagation indicate further works are needed to clarify the consequences [52]. Iron-oxides can have an effect on GPR signal propagation, especially in the Martian regolith different water content is expected to occur according to seasons, what should be considered.

Identification of bulk liquids water might be moderately straightforward [53], as it absorbs the radar signal – but water could be rare or absent on Mars today. There is an ongoing debate on the possibility of liquid water existence in the subsurface. Recently MARSIS data based high basal reflectivity of the South Polar Layered Deposits (SPLD) was identified, being consistent with liquid water [54] under 1.7-km-thick ice layer, however salty ice as could explain the observation [24]. Considering the liquids in the Martian subsurface perchlorate brines might form in the shallow subsurface at high northern latitudes [55], where grain size related adsorption plays a strong role, producing up to 0.5-1 wt % adsorbed water in the low and mid-latitudes [56]. Specific analysis by the Dynamic Albedo of Neutron (DAN) instrument onboard NASA's Curiosity rover the abundance of water and chlorine Gale crater was measured, and Water-equivalent hydrogen (WEH) values showed variability between 2 and 3 wt% [57] there. Further indirect indications could come from the influence on impact ejecta distribution both regarding ejection angles and velocities (Aleksandra et al., 2024), and by future seismo-acoustic method to characterize subsurface water on Mars [58]. Related subsurface ice distribution was mapped under the SWM (SUBSURFACE WATER ICE MAPPING) project [59], and using theoretical considerations [60], Martian water budget indicates about 30–90 % of the missing Martian water resides below the surface.

However, considering few or no **subsurface liquid water,** the radar signal could penetrate much deeper on Mars than in the case of the Earth. To optimize the methodology for conducting "real deep" surveys on Mars, it would be beneficial to perform tests in desert locations or wintertime "deep" permafrost regions on Earth. However, the elevated abundance of iron containing minerals on Mars could potentially affect the interpretability of GPR signal. Some calculations suggest that the signal attenuation caused by highly magnetic minerals [61] could still be too small to allow the recording of useful data [62] on Mars. Understanding the presence and the amount of magnetic minerals is also important to help in paleo-environment reconstruction, and their indication using radar through attenuation and backscattering measurements could also be investigated. In general, longer radar wavelengths

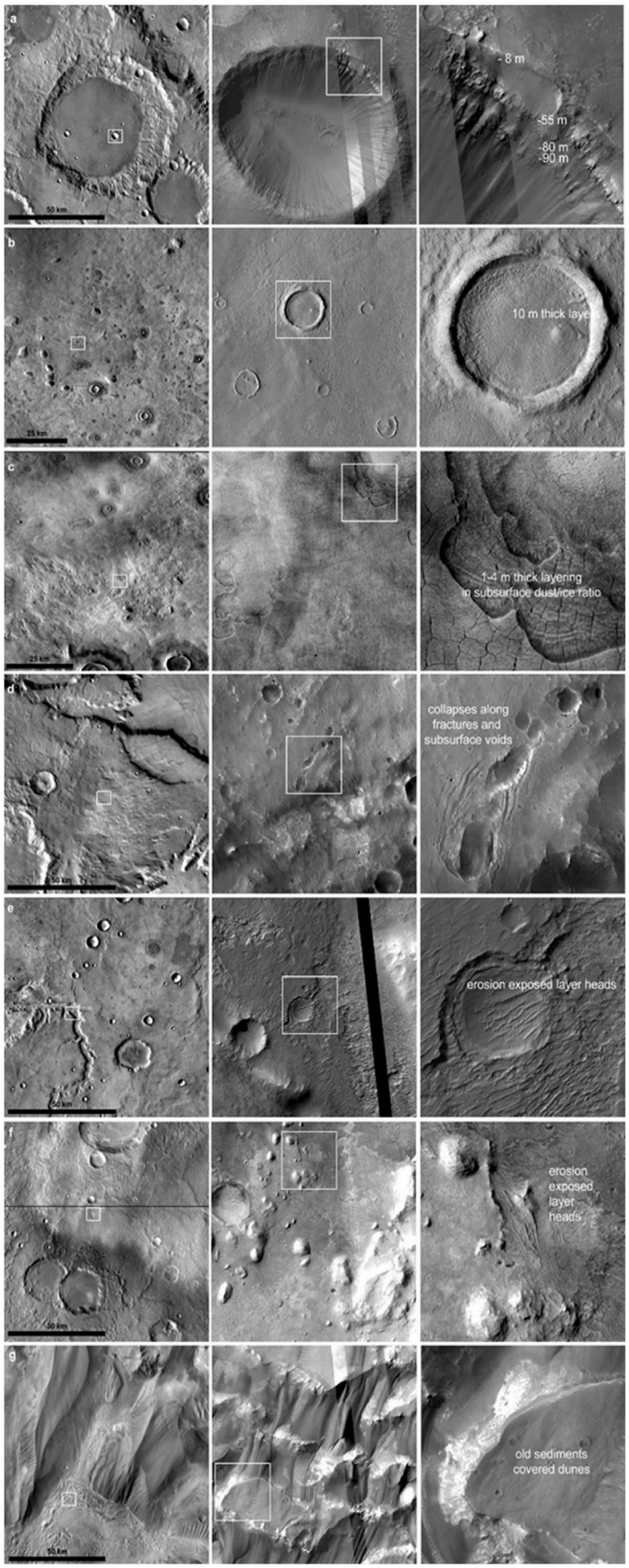

Fig. 2. Surface exposed shallow subsurface structures on HiRISE images. Lines correspond to lines (and panel no.) in Table 3. First column shows 100 km diameter terrain using THEMIS images for context, second column shows about 4 km diameter part of the HiRISE images, while third column shows 1×1 km magnified section of the images.

are more suitable for conducting surveys in targets with magnetic minerals like expected on Mars, as lower frequencies are less affected by attenuation and can penetrate deeper into the subsurface.

Although several minerals on Mars show widespread **hydration** [63–66], the radar wave attenuation by the hydrates state is expected to be minimal in absence of bulk liquid state, making it challenging to identify them by GPR. However, this area of research is still poorly understood and there could be possible important targets, such as deeply buried clays and other minerals that could have retained their hydration state for billions of years under the cold Martian environment with limited tectonic and volcanic activity.

The following are some interesting materials that are expected to occur on Mars and can be targets for GPR analysis.

- **Regolith** with loose sand and silt – basaltic bedrock contact is an interesting target for GPR survey on Mars. In this scenario, scattering is expected to decrease as the grain size become smaller, and the bedrock becomes less porous with depth. The GPR signal is expected to exhibit possible volume scattering in the near-surface region, which may diminish with increasing depths.
- Formerly **cemented duricrust** (iron oxides filled voids between regolith grains or hydrated weathering products) – loose uncemented debris. Such setting is expected to occur around the top decimeters in the shallow subsurface ([67,68], Souness et a. 2016), or deeper at former surfaces that later got covered. These settings might be produced by microscopic water condensed from the atmosphere or by water uptake of minerals from surface ice under past climates. Here the change of air filled porosity together with ideally observable GPR signal change from weathered minerals might occur jointly. Based on the tests of Bierson et al. [69], OH bearing clay minerals or saline ice can also produce such dielectric permittivity contrast what could be observed by GPR using specific wavelength, including the case of MARSIS measurements [54,70].
- **Snow or ice** – dry silicate debris contact from earlier or recent climate change deposited snow (partly covered by with driven dust) could emerge at many locations in the middle-latitude region. Such settings are expected to occur within the top 1 m at latitude dependent mantle (LDM) covered terrains or within several meters of depth at Viscous Flow Features (VFFs), both from the roofing upper and bottom silicate, separated by an ice layer between them. Such settings have been partially observed by SHARAD at several locations in the middle-latitude region of Mars [71,72]. Considering the presence of **microscopic liquids**, it is possible for small-scale salty liquid brine to emerge at ice/mineral interfaces. These brines are likely formed under different past climates, where hygroscopic salts bind the H_2O content, resulting in microscopic brines filling the voids between the silicate grains. Lower-frequency radar signals are more effective than high frequency signals in identifying changes in fluid salinity ([73].)

There is an important aspect to consider regarding the separation of buried ice and buried loose porous material where loss tangent value could be the same. However, the loss tangent of water ice increases much with temperature [74], affecting the attenuation of the radar wave. While the loss tangent of pure water ice and water ice - dust mixture is quite similar above 230–240 K [75], but show a strong difference below this range. Under the current expected shallow subsurface temperatures on Mars, values below 230 K are expected to be around 208 K, and even lower at higher latitudes. This means the loss tangent difference between pure and dusty snow/ice is around the scale is 0.0001 around the equator, while getting somewhat larger at higher latitudes – however the required exact detection might be a challenge.

4.1. Size of geological features

Based on the existing data on various surface features on Mars (Hargitai and Kereszturi 2015), Table 4 provides a list of basic observable characteristics, while Table 5 indicates the typical physical dimensions. While the outcrop or collapsed openings of these features are sometimes visible on the surface, they extend into the subsurface. These deeper buried sections, which are inaccessible to current detectors, contain valuable information for paleo-environment reconstruction. These regions could be effectively targeted using the proposed FlyRadar category instrument.

There is a range of expected geological features in the top 20 m deep subsurface region (Table 5), which may be identified for the first time by the proposed radar. To ensure reliable interpretation of data, the radar survey should cover horizontal distance on the scale of km. This would not only enable further confirmation and identification of the features, but also facilitate their correlation to the regional context and geological history. By conducting traverses along specific features, lateral changes can also be identified, revealing variations in fluvial or lacustrine sedimentation, preferred regions for snow/ice accumulation, lava cave routes Such lateral changes could provide unique information for paleoenvironmental reconstruction.

In the case of geological structures listed in Table 5, surface traverses by rovers are not feasible due to the steep terrains such as fluvial channel interior, deposited bars at channel termination, sedimentary delta front eroding outcrops surrounded by fallen off boulders, or lava caves. High resolution analysis of these hazardous terrain types cannot be performed by rovers; it can only be achieved safely through drone based GPR methods.

Table 6 summarizes the expected radar-based observations in the shallow subsurface of Mars. In terms of spatial resolution at the ground level, the selection of the drone flight altitude is crucial. For example, considering an altitude of 100 m, the cross-track resolution would be around 20–30 m and 5–10 m in along track when applying unfocused processing. These resolution values would be sufficient to survey and map the target types listed. Considering the general aspects, it is expected that shallow (few meters deep) targets are abundant on Mars. Due to the overall aridity and low temperature on Mars, humidity levels are expected to be low, enabling deep signal penetration. However, the presence of magnetic minerals poses a challenge in GPR analysis. Nevertheless, the abundance of ice in the shallow subsurface suggests the existence of numerous ideal targets, despite the potential increase in attenuation and scattering caused by magnetic minerals.

The targets and their characteristics listed in Table 6 show that different strategies could be determined and shaped according to the targets, where well selected airborne drone based GPR routes are expected to gain new results. During the design of the strategy, analogue structures on the Earth should be tested and routes to be improved during field works, as such activities have already been started recently.

4.2. Knowledge gaps to uncover

Fig. 3 below further shows the groups of various target types with context, and the “gap” in the middle of the vertical axis. This shallow 10–50 m subsurface region represents the next logical step in the development of in-situ Mars research, and also for the development of ISRU possibilities to support the planned human mission.

Radar properties can be utilized to estimate safety aspects related to specific terrains on Mars. These include determining the thickness of loose aeolian dust on the surface, assessing the stability of the shallow subsurface for rover traversing, and identifying the easiest drilling locations in terms of hardness and porosity. In addition to identifying important subsurface targets for research, aerial surveys using radar can help evaluate access possibilities, particularly for drilling to access water ice, by identifying the shallowest occurrences.

4.3. Technology related aspects

Based on the overview presented in this work, there are key **future**

Table 4
Summary of some general expected properties of various target types on Mars.

Feature	Characteristics and occurrence on Mars	Observable properties by GPR	Earth or laboratory analogues
Porosity change	Downward decreasing porosity in general, poorly cemented sand layers and possibly ones by iron-oxides and hydrated salts near the surface (duricrust)	Cavity, air filled porous voids detection, which are good radar reflectors however difficult to interpret as the size of voids matter much, evaluation of sediment compaction in general	Differently compacted snow/firn/glacier ice (Hickson et al., 2018)
Compositional change	Mineral composition change at sedimentary terrains (sulphates, chlorides, iron-oxides, carbonates, clay minerals)	Different permittivity compared to the most abundant basaltic material, although expected to be small differences regarding mineralogy, texture and temperature, but and poorly quantified	Laboratory based dielectric models (Brouet et al., 2019) including meteorites [76]; temperature effect (Stillman 2008); analyzing propagation using simulants [62]
Liquid water or brine occurrence	At shallow subsurface might occur only at high salt content and at proper temperature	Velocity of signal provides estimate of SWE (snow water equivalent) using Earth based experiences [77], estimating the presence of small water inclusions [78]	Ground truth (Abazagana 2020) support to convert the measured dielectric permittivity to water content using the dielectric mixing model [79]; recently developed methods to interpret multiple scales heterogeneities and 3D porosity model [80]
OH content change	Might increases downward at low latitude sites, elevated at mid- and high latitude sites even close to the surface, however buried OH containing material could occur at many locations	Using Earth based analysis of 500 MHz center frequency pulsed radar, the variation in clay content (main OH host mineral group) might shift of the frequency of spectral peaks [81], however might be difficult to identify	Laboratory testing with specifically selected mineral components, field tests at clay bearing permafrost [82]
Ice occurrence change	Same as above, might occur at small depth if buried, definitely occurs at mid- and high latitudes	Internal boundaries at density changes, water or solid sediment content could be observed; permittivity contrast between ice and liquid water, allows the identification even small amount of liquid water by altering the dielectric constant [83]	High latitude permafrost terrain and buried ice interbedded with sand, including niveo-aeolian dunes [84] and polar caps [85]
Rock hardness	Compaction and mechanical resistance	Correlation between mechanical properties and permittivity might exist	See ElShafie et Heggy 2013, however further are tests are needed
Structural change	Occurrence and orientation of micro-fractures	Faults, fractures could be identified however they make dispersion attenuation and related uncertainty – their proper interpretation requires improved algorithms [86]	Field analogues analysis of fractured rocks on the Earth (Meideros et al., 2018)
Heterogeneities	Boulders, cavity, regolith base etc.	Hyperbolas of diffractions	Shallow subsurface rock detection [87]

Table 5
Overview of the size of various potential target features. The second column marks the expected origin of the dielectric contrast between the given feature and the "average" regolith located below.

Feature	Target GPR properties	Dielectric contrast	Size range	Depth range
Fluvial channel, former riverbed	Bedload, small grains sediment	Moderate	100 x 5 km	2–20 m
Buried snow/ice layers	Different dielectric constant of ice and pores also (if exist)	Strong	10–100 km	1–20 m
Buried dunes	Porous, weak scattering interior	Moderate	10–300 m	0.8–15 m
Former surfaces (duricrust)	Small grains made up, but occasionally cemented unit	Moderate	10–100 km	0.5–1 m
Hydrated surface units	Elevated OH content, weakly observable	Weak	10–100 km	1–2 m
Lava caves	Air filled voids, very large contrast	Strong	10 x 0.05 km	1–10 m
Ridges	Discontinuities, deformed layers, scale of displacement	Weak	1–10 m	1–10 m
Volcanic products	Ratio and spatial setting of lava vs. pyroclastic units, lava unit sequences	Moderate	0.1–100 km	1–50 m
Former crater lake sediments	Different grain size and pore filling chemical precipitates	Moderate	10–100 km	1–5 m

directions for improvement that could be outlined. One crucial aspect is the development of modelling approaches and/or the expansion of knowledge to enable the estimation of specific parameters beyond what is captured in the radar echoes. A significant challenge lies in conducting **robust geological analysis** to estimate the mineralogy and lithology of the shallow subsurface. However, this task may be more feasible in the targeted 10–50 m shallow layer compared to deeper locations that are the focus of SHARAD or MARSIS. A specific Mars relevant feature of the surface is the regolith, and its thickness could be estimated by thermal inertia (top dm layer e.g. the thermal skin depth) and stratigraphic

Table 6
Expected findings and strategy for GPR targets (* marks two possible similar features and their properties).

Group	Target geological features	Expected observable characteristics	Expected strategy and findings by FlyRadar category GPR observations
Volcanic	Lava tubes (Qui and Ding 2023, Crown et a. 2022)	Dielectric contrast in subsurface voids and various objects accumulated there (like fallen rocks or condensed ice)	Aerial survey starting from skylight openings, where beside the existence and spatial distribution, even internal collapse features, possible climate change related shielded ice accumulation
	Pyroclastic vs. lava flow products [88]	Large porosity difference, shape of interfaces, stratigraphic sequence of units	Separation of explosive and effusive eruption produces, volcanic process identification (flow/ tephra fall/debris surge/ autobrecciation), volatile estimation of magma, surveying structures at candidate volcano/ice interaction regions
	Lava flow or pyroclast units [89]	Lava unit interfaces, separation of buried subsurface units, volume calculation	Eruption volumes, episodic/recurrent activity, volcanic gas content estimation from porosity along pre-defined "ideal" tracks
Icy features	Latitude Dependent Mantle* (Schon et a. 2012)	Thickness of ice-dust mixtures, internal dust distribution and mixing ratio	Confirmation of the existence of ice-dust mixture, reconstruction of melting events (gullies), cleanness of ice, paleo-climate proxy, survey at mid-latitude zones of LDM morphology
	Bulk ice in VFFs [90,91]	Ice/rock interface, bulk ice porosity, layering, ice thickness at <100 m depth	Deposition of ice, improve conditions necessary for glacial creep, origin and characteristics of debris cover, improved sublimation/retention modelling, paleo-climate proxy, by survey at glacier like forms (GLF), Lobate debris aprons (LDA), lineated valley fills (LVF), concentric crater fills (CCF)
	Dust covered shallow ice at middle-high latitudes* [92]	Separation of buried ice masses, estimation of their dust content, areal distribution	In-situ resource utilization (ISRU) usage possibilities, connection between ice distribution and surface features plus preferred locations, paleo-climate proxy, should be targeted by aerial survey defined using surface morphology with feedback of surface-subsurface connection being revealed during the survey
Water related features	Gilbert-like deltas [93]	Interfaces of topset/ foreset structures, porosity distribution	Rough grain characteristics sedimentary facies, confirmation of ancient standing water bodies, cyclicity of inflow, paleo-climate proxy, by survey tracks crossing the frontal edge of the delta
	Subsurface source regions of chaotic terrains	Subsurface faults, depth of fragmented layer, morphology or redeposition	Source of outbreak water, process of collapse after the event, volume of released H_2O, signs of ponding, related paleo-climatic extrapolation
	Bottom of former crater lakes	Interface and grain properties to define sedimentary aspects	Separation of former lakebed sediments from other materials, signs of ancient waves, shallow sub-lake mass movements, by several quasi parallel traverses from the bank toward the former lake interior
	Possible occurrence of subsurface brine layers at salty locations	Strong echo from liquids, linking them to local stratigraphy	Identification of possible shallow brine layer, role of temperature and salt on brine emergence, information on local context to fit to the regional stratigraphy, survey to identify the spatial extent of subsurface liquid
Sedimentary features	Interior Layered Deposits (Flahaut et a. 2010)	Layer interfaces, morphology of former surfaces	Internal structure, erosion and deposition characteristics, information for their origin, signs of former surface ice condensation by surveys crossing probable different facies
	Mass wasting features	Interfaces, size of slumped blocks and debris	Formation conditions, linking to climatic and other sources, by survey perpendicular to the movement direction
	Duricrust and cemented regolith	Different porosity of the regolith, separation of subsurface layers	Estimation on chemical alterations, linking to the role of possible brines or ice deposition driven chemical processes, ice or microscopic brine formation locations
	Dune interiors	Distribution of porosity, internal inhomogeneity, layering, void fillings	Possible ice (or sulfate, iron-oxide) cementation of dunes, deposition conditions, climatic proxies

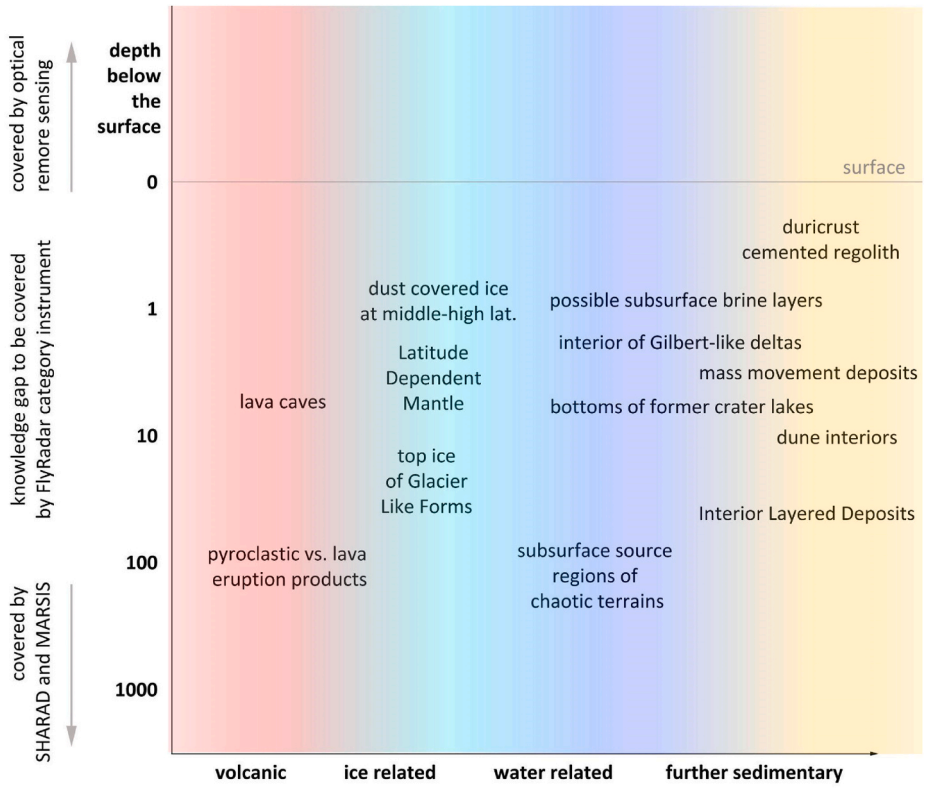

Fig. 3. Schematic overview of various subsurface features considering the used (or planned) wavelength of survey (vertical axis) and the geological theme the given feature is connected to (horizontal axis).

analysis (by outcrops, regarding the top few m layers probably).

The **permittivity estimation** has probably the largest uncertainty in the interpretation of subsurface reflections. This difficulty might be partly overcome by extrapolation using context geology and especially stratigraphy, partly at steep outcrops nearby. However, the porosity and structural aspect could be difficult to estimate, while the occurrence of exposed snow or ice, as well as some specific sedimentary features might be more easily identified in favorable cases.

Based on a rough estimate of the **average permittivity** from diffraction hyperbola, in a next step the thickness variation of the regolith could be estimated, while in a second step the time delay and reflected energy could be used for a finer estimation using the context information on stratigraphy. This process would benefit from the availability of multiple radargrams from different terrain types on Mars (like continuous bedrock based on outcrops, porous tuffs at heavily eroded volcanoes, ice cemented material at ice outcrops on slopes etc.), to strengthen the interpretation by comparing these end cases to each other. It is important to note that this iterative process will require the accumulation of more established knowledge as data becomes available. Another advantage, compared to Earth, is the expected scarcity of moisture in the subsurface, which allows deeper penetration and clearer echoes, facilitating the interpretation of such parameters like porosity, voids, structural features etc. there. Using permittivity estimation it will be possible to have a good estimation of underground geometry.

Despite the challenges related with the interpretation of observations, there are several possibilities for improving the **reconstruction** of the subsurface settings. One possibility is the correlation between the porosity and thermal inertia, which can help to estimate the topmost porosity (down to the daily thermal skin depth, what is usually <1 m). Using this approach, linking thermal based shallow porosity data to stratigraphy, gradual improvement could be done during the running of the observations. Additionally, the survey of the same targets from different directions can also increase the accuracy, especially in identifying compositional differences and target shape. A further important possibility what could provide new results among the findings is the connection between target rock specific mechanical property and GPR response. Based on recent works there is a possible connection between the dielectric constant and rock hardness [94], however further laboratory tests are needed here.

A Mars drone-ready GPR instrument offers several advancements compared to existing technologies. It provides enhanced mobility and accessibility, allowing access to remote and inaccessible areas on Mars that are not easily or dangerous to reachable by rovers. This enables exploration and surveys diverse geological settings, make rapid surveys, mapping and large areal coverage in a short period. This capability facilitates efficient mapping and surveying of extensive regions. With advanced signal processing algorithms and improved hardware, it can collect high resolution data subsurface features opening the possibility to better reconstruct the geological history. Drones also offer the flexibility to allow multi-temporal observations by conducting repeated surveys of the same region at different times, including daily and seasonal cycles, revealing volatile changes – discovering the dynamical nature of Mars.

Ideal trade-off between frequency - spatial (both horizontal and vertical) resolution - penetration depth should be further evaluated, including larger antenna for larger penetration. The choice of a frequency around 100 MHz is due to several practical considerations, including the physical size of the antenna, what is inversely proportional to the operating frequency. For drones there are limitations on the size and weight of the antenna that can be carried. Therefore, a 3 m wavelength offers (100 Mhz frequency) a good balance between resolution and penetration depth. Scattering effects, which can influence the quality of the GPR signals, what are reduced when compared to higher-frequency GPR systems like WISDOM, enabling clearer and more interpretable subsurface images.

Additionally, at these wavelengths, the attenuation of the electromagnetic waves in the Martian subsurface is still acceptable, based on the estimation of the attenuation at frequencies of SHARAD and

MARSIS. Considering that the attenuation is related to the operative frequencies, we can expect the GPR signal to exhibit an attenuation (in dB) that is about few times higher compared to SHARAD data (in decibel scale: $K = 27\ f \tan \delta$. However, despite this higher attenuation, the signal-to-noise ratio (SNR) is expected to be larger, which compensates for the increased attenuation. As a result, the maximum penetration depth of the GPR signals could be not so far from that of the SHARAD system, with the potential to penetrate several tens of meters or even hundreds of meters (depending on the loss tangent of the subsurface materials) before experiencing significant weakening.

4.4. Technology of the used breadboard

Beside the evaluation of the targets and the expected performance of GPR signal on Mars, a breadboard to test drone based GPR on the Earth is being developed by the authors of this work. Although the aim of this paper is not the technical specification of this breadboard, however a short summary is presented below to provide insight the characteristics of such a system to orient related future works.

The UAV used for tests is a Tundra built by the Hexadrone Company, what is an X-shaped quadricopter modular drone, which allows it to adapt to various payloads. The wingspan from motor axis to motor axis of the Tundra is 1100 mm with four carbon blades of 280 mm. It is capable of lifting a payload of more than 4 kg with a maximum of 8 kg including the batteries with a flight duration of 30 min. It utilizes a Pixhawk 4, with an Herelink radio system running in the 2.4 GHz band, capable of streaming two HDMIs signals. The UAV is equipped with a 2.4 GHz Wifi transmitter receptor for communication with the base station at more than 2 km, allowing to transmit and receive more than 20 MBit/s. A tension regulator ensures a constant voltage to the radar under different fight conditions.

All parts of the electronic hardware are arranged into two units: the Ettus E320 board and the R86S mini computer. The Ettus E320 board represents the cutting edge of SDR (Software-Defined Radio) technology equipment used for the software synthesis real time processing, while the R86S computer performs the control and storage functions. The next-generation SDR card uses Analog Devices' AD9361 flexible 2x2 MIMO transceiver, which covers frequencies from 70 MHz to 6 GHz and provides up to 56 MHz of instantaneous bandwidth. The open source USRP Hardware Driver (UHD) API and RF Network-on-Chip (RFNoC) FPGA development framework integrated with standard development tools such as GNU Radio. The baseband processor uses the Xilinx Zynq-7045 SoC and a dual-core ARM CPU and Linux operating system with high-speed interfaces of 1 Gigabit Ethernet.

The system utilizes two Yagi-Uda antennas single polarization for sounder mode and two log-periodic antenna, two polarization for SAR mode. The working frequencies are 80 MHz for sounder mode and 450 MHz for SAR mode. The total electrical need is 35 W, given by drone batteries, and the weight of the antenna is about 0.8 kg each. The total envelope for the radar electronic box is 180x110 × 85 mm with a total weight of about 1.7 kg. Comparing these values to those suggested for the Mars Science Helicopter (MSH) project (Joahan et al., 2022) which has two design versions. The smaller one is a coaxial helicopter design, planned to realize 2–10 km/sol long surveys up from 1 to 2 km altitude, with a payload capability about 1–5 kg. This MSH version is close to the one outlined directly above under the project running by the authors of this work. The MSH aims a bit deeper subsurface survey, and focus on the 10–100 m deep layer, while the above mentioned design, as well part of the outlined targets have more focused aspects in a somewhat shallower 1–20 m deep zone – however large overlap is present between the two concepts. The goals of MSH mission would be to find organics associated with clay-bearing or silica-rich units, search for ancient sediment contains biosignatures, with mapping geologic units, identify sampling locations, and deliver geologic material to the landed platform for further analyses. However the concept and targets outlined in this work aims more general geological survey that provides background but not directly focuses on astrobiology relevant aspects.

Considering technology related limitations, based on the current capabilities of batteries, a drone that carries an average capacity battery could not fly long distance continuously on Mars but only on the scale less than 1 h. During the Ingenuity mission a flight distance of ~17 km and during >2 h for comparison [95], however Ingenuity was a very light drone. Calculating with the fly speed of Ingenuity around 30 km/h, a future drone with similar capacity could survey 10–20 km during one flight. Having similar solar panels as Ingenuity, after one flight roughly one Martian day is needed to recharge the battery. Thus a 100 km traverse could be surveyed by 10–15 Martian days. On this two week scale of period, several such surveys could be realized on an average mission with around one Martian year lifetime. Considering the size range of potential targets listed in Table 5, most of the features could be crossed at least one time but more probably 2–3 times during these 10-15 Martian days, e.g. for a one Martian year mission larger than a dozen traverse could be realized for several target structures.

Further challenges for a GPR survey hosting drone could face on Mars are discussed below. Interference of **surface clutter** affects the target detection and interpretation of radargrams substantially. Information on the density of the top few cm thick layer could help to better consider and decrease the consequences of surface clutter. The global dataset from the THEMIS orbital instrument based thermal inertia (TI, [96,97]) provides a rough estimation on the density, and could be used to improve permittivity and propagation speed estimations, just like the determination of mineralogy from orbital data. High resolution DTMs are partly available for Mars and could be used to simulate the surface echoes and hence support the clutter related improvement.

As the target depth considered in this work is moderately shallow (few meters), high spatial resolution DTMs are needed. Using proper HiRISE stereo image pairs, around or somewhat better than 1 m spatial resolution could be achieved, but for ideal situations the drone that carries the GPR should record stereo image pairs along the target stripe, and easily achieve a few cm spatial resolution from the 10–50 m flying altitude. Surface roughness could be also better determined by drone than orbital data, however it plays a smaller role in the reflectivity and signal transmission inside, affecting the estimation of signal power – however might have visible impact if the scale of roughness is close to the used wavelength. The consequence on clutter emergence is usually negligible compared to the coherent clutter reflected from the surface, but under specific conditions, the scale roughness could be easily acquired and used for the simulations. Finally new possibilities along with the improvement of digital technology like clutter removal by neural networks (Dun et al., 2022), multi-resolution and multi-directional information, as well as adaptive dictionaries and novel regularization strategies support to gain clearer radargrams. However heterogeneity of the regolith presents a challenge, what is poorly known for Mars [98].

Another critical aspect is the positioning of the drone, keeping its **elevation and attitude** during the radar survey. The flying altitude of the drone could be easily modified and adapted up to 200–300 m without expected technical difficulties. Although the emergence of atmospheric vortex features below the planetary boundary layer (about 10 km on Mars, [99]) is expected to increase toward the surface, their scale and frequency is poorly known yet. Currently dust devils are already observed in the lower atmosphere of Mars, which emerge frequently around noontime at middle and low latitudes, but do not seem to show very high spatial density – however their possible automatized avoidance might be useful for future drones for safety aspects. Lower flying altitude allows a survey to achieve higher spatial resolution and better S/N ratio, but covering a more narrow swath. The optimal flying altitude should be a tradeoff between energy – safety – achievable data quality; and the expected spatial characteristics of the target. Here identification of subsurface stratigraphy changes (like edge of former lake sediments or fluvial channel cross sectional profiles) would favor lower altitude and narrower band to survey, while targets with "areal interest" like an extended delta deposit, area of past

hydrothermal activity or divergent branches of lava caves) might favor larger flying altitude with larger area of covered stripes.

Keeping of attitude requires compensation of side winds produced tilting and shaking of a drone, what might require resemble mitigation methods like used on the Earth for flying drones under windy conditions. In these aspect more theoretical than practical real life solutions have been published recently [100], where underactuation (case of manipulator which has less actuators than the number of joints) of free floating robots [101] seems to be a general aspect waiting for solutions. Algorithms that support drone positioning (especially Aerial Manipulator control system [102], but also Dynamic Image-based Visual Servo Control, Fault Tolerant Control, Finite-time Control, NMPC, Nonlinear Optimal Control) are developing fast, might became mature until a GPR hosting drone will fly on Mars. Obstacle avoidance is not a main issue at moderately flat terrain, however position determination requires a fixed ground station with direct radio/WIFI contact toward the drone. Earth based drone flying experiences indicate moderately stable attitude is expected below 4–8 m/s wind speed [103], what is around the scale of the often measured 1–4 m/s by Viking landers, while 15–25 m/s inferred from Ingenuity movement [104], while much less in disturbance is expected than on Earth at same wind speed because of the rare atmosphere of Mars. Decision on flying on a specific day would require the comparison of wind resistance of the drone [105] and meteorological measurement plus modelling based wind speed forecast.

5. Conclusion

The possibility and feasibility of future drone-based shallow subsurface GPR radar survey for Mars have been examined. The discussed capabilities were found to be relevant for the planning of next missions to survey the top 50 m subsurface layer for science and ISRU activities. Evaluating SHARAD based somewhat deeper subsurface regions provided a range of useful findings already, while HiRISE based analysis of outcrops indicates there are several target features in the shallower subsurface region, waiting for discovery.

Sedimentary and volcanic environments are the most common geological settings that are expected to show interesting variability in the shallow subsurface. Based on the results gained in this work, the main scopes and knowledge gaps that should aim an airborne shallow subsurface radar survey on Mars, are the following **targets**: ice content of indurated dunes, including those that present nivean features, internal layering of fluvial deposits, including delta like structures, mid- and high latitude ice containing features to provide constraints for recent climate changes, including GLF, LVF, LDA, CCF [106] as well as shallow buried snow/ice layers exposed at steep slopes, former crater lake sediments, lava caves and possible ice content there.

The proposed FlyRadar category instrument will have to be able to explore discontinuities in the underground to measure thickness, volume and stratigraphic sequence. Evaluating the expected size of various geological structures, crossing of 100–1000 m sized geological features, it is expected that such information will be gained what is not available targeting only the surface. Directions of later buried and poorly visible lava flow routes could be determined only using earlier surveys but not with a rover of limited traverse capability and inability of crossing any terrain type on the surface.

The permittivity of the investigated subsurface units should be estimated to get values of porosity and density of the target rocks. This data will help to classify the geological environment and the rock nature. Moreover, very high resolution images of the Martian surface serve as a base to define the possible size and geometry of potential target features. As the presence of liquid water is very rare or does not exist in the Martian crust currently, the FlyRadar instrument will be able to operate over most of the Martian surface.

Radar penetration depth and signal clarity could be increased by the low humidity that is expected in the Martian subsurface, while the probable abundance of metals mainly in iron-oxides of the regolith could decrease the signal with scattering effect. As radar signals are strongly affected by the presence of liquid water that is very common on Earth, the FlyRadar instrument will be tested mostly in dry areas that are arid hot deserts, karsts or cold arid areas where water is frozen.

At high frequencies optimum vertical resolution accompanied with low penetration depth, while at low frequencies with worse vertical resolution the signal will reach a greater depth. Thus, a tradeoff has to be defined according to the geology of the investigated areas. As a result, to compromise between the possibilities and moderately easy realization, for the survey of the top 50 m of subsurface layer on Mars could be done at 20 MHz of bandwidth with 80 MHz of transmitted frequency ($B/f = 1/4$). The mass of such an instrument should be decreased, however it looks realistic that an order of kilogram mass payload could provide all the needed capabilities in the near future. The drone technology also seems to be realistic and available to do such survey-like research at 10 km scale distances, what neither an orbiter nor a surface rover could achieve, using for example with the planned Mars Science Helicopter [107]. The proposed instrument category and capacities would be an important next step for Mars research and human exploration.

CRediT authorship contribution statement

Akos Kereszturi: Writing – original draft, Conceptualization. **Gian Gabriele Ori:** Funding acquisition, Conceptualization. **Nicole Katerin Dias Marques:** Formal analysis, Data curation. **Philippe Grandjean:** Investigation. **Pascal Allemand:** Formal analysis, Data curation. **Vilmos Steinmann:** Formal analysis, Data curation. **Gianni Alberti:** Formal analysis, Data curation. **Marco Mastrogiuseppe:** Formal analysis, Data curation. **Joanna Gurgurewicz:** Methodology, Investigation, Conceptualization. **Wlodek Kofman:** Investigation, Conceptualization. **Daniel Mège:** Conceptualization. **Claudio Orlanducci:** Formal analysis, Data curation. **Pierre-Antoine Tesson:** Investigation. **Osip Kokin:** Investigation, Data curation. **Sylvain Augier:** Formal analysis, Data curation.

Declaration of competing interest

The authors declare that they have no known competing financial interests or personal relationships that could have appeared to influence the work reported in this paper.

Acknowledgement

This project FlyRadar has received funding from the Europian Union's Horizon 2020 research and Innovation Programme MCSA Rise 2020, Grant Agreement No. 101007973. The support as Internal fund from Thales Alenia Space Italia is also acknowledged.

References

[1] Keck institute for Space studies (KISS), in: C.J. Culbert, B.L. Ehlmann, A. A. Fraeman (Eds.), Revolutionizing Access to the Mars Surface. Final Workshop Report for the W.M, Keck Institute for Space Studies, Pasadena, CA, 2022, https://doi.org/10.7907/d1sm-mj77, 2021.

[2] R. Jordan, G. Picardi, J. Plaut, K. Wheeler, D. Kirchner, A. Safaeinili, W. Johnson, R. Seu, D. Calabrese, E. Zampolini, A. Cicchetti, R. Huff, D. Gurnett, A. Ivanov, W. Kofman, R. Orosei, T. Thompson, P. Edenhofer, O. Bombaci, The Mars express MARSIS sounder instrument, Planet. Space Sci. 57 (2009) 1975–1986.

[3] G. Picardi, et al., in: A. Wilson, A. Chicarro (Eds.), Mars Express: the Scientific Payload SP-1240, ESA, Noordwijk, 2004, pp. 51–69.

[4] R. Seu, R.J. Phillips, D. Biccari, R. Orosei, A. Masdea, G. Picardi, A. Safaeinili, B. A. Campbell, J.J. Plaut, L. Marinangeli, S.E. Smrekar, D.C. Nunes, SHARAD sounding radar on the mars reconnaissance orbiter, J. Geophys. Res. 112 (2007). IssueE5, E002745.

[5] E.R. Jawin, B.A. Campbell, J.L. Whitten, G.A. Morgan, The lateral continuity and vertical arrangement of dust layers in the martian north polar cap from SHARAD multiband data, Geophys. Res. Lett. 49 (2022) e99896 article id.

[6] C. Li, Y. Zheng, X. Wang, et al., Layered subsurface in utopia basin of mars revealed by Zhurong rover radar, Nature 610 (2022) 308–312.

[7] S. Nerozzi, J.W. Holt, Buried ice and sand caps at the north Pole of mars: revealing a record of climate change in the cavi unit with SHARAD, Geophys. Res. Lett. 46 (13) (2019) 7278–7286.

[8] Colin M. Dundas, Michael T. Mellon, Susan J. Conway, Ingrid J. Daubar, Kaj E. Williams, Lujendra Ojha, James J. Wray, Ali M. Bramson, Shane Byrne, Alfred S. McEwen, Liliya V. Posiolova, Gunnar Speth, Donna Viola, Margaret E. Landis, Gareth A. Morgan, Asmin V. Pathare, Widespread exposures of extensive clean shallow ice in the midlatitudes of mars, J. Geophys. Res.: Planets 126 (3) (2021) e06617 article id.

[9] J. Mouginot, A. Pommerol, P. Beck, W. Kofman, S.M. Clifford, Dielectric map of the Martian northern hemisphere and the nature of plain filling materials, Geophys. Res. Lett. 39 (2012) L02202, https://doi.org/10.1029/2011GL050286.

[10] N.L.G. Schiff, T.K.P. Gregg, Probable ice-rich deposits on north-facing slopes in Alba Patera, Mars, Icarus 383 (2022) article id. 115063.

[11] G.A. Morgan, N.E. Putzig, M.R. Perry, et al., Availability of subsurface water-ice resources in the northern mid-latitudes of Mars, Nat. Astron. 5 (2021) 230–236.

[12] Sigurd Eide, Titus M. Casademont, Tor Berger, Henning Dypvik, Emileigh S. Shoemaker, Svein-Erik Hamran, Radar attenuation in the shallow martian subsurface: RIMFAX time-frequency analysis and constant-Q characterization over jezero crater floor, Geophys. Res. Lett. 50 (Issue 7) (2023) e2022GL101429 article id.

[13] Xiaotian Li, Wei Yao, Hao Wang, Martian subsurface water ice prediction at the Tianwen-1 mission landing site, Icarus 389 (2023) 115268.

[14] T.M. Casademont, S. Eide, E.S. Shoemaker, Y. Liu, D.C. Nunes, P. Russell, H. Dypvik, H.E.F. Amundsen, T. Berger, S.-E. Hamran, RIMFAX ground penetrating radar reveals dielectric permittivity and rock density of shallow martian subsurface, J. Geophys. Res.: Planets 128 (5) (2023) id. e2022JE007598.

[15] Emileigh S. Shoemaker, Titus M. Casademont, Lynn M. Carter, Patrick Russell, Henning Dypvik, Sanna Alwmark, Briony H.N. Horgan, Hans E.F. Amundsen, Sigurd Eide, Svein-Erik Hamran, David A. Paige, Sanjeev Gupta, Emily L. Cardarelli, Uni Árting, Tor Berger, Sverre Brovoll, Observations of igneous subsurface stratigraphy during the jezero crater floor rapid traverse from the RIMFAX ground-penetrating radar, The Planetary Science Journal 5 (8) (2024) 27, id.191.

[16] L. Zhang, C. Li, J. Zhang, et al., Buried palaeo-polygonal terrain detected underneath utopia Planitia on mars by the Zhurong radar, Nat. Astron. 8 (2024) 69–76.

[17] Ling Zhang, Yi Xu, Renrui Liu, Ruonan Chen, Roberto Bugiolacchi, Rui Gao, The dielectric properties of martian regolith at the tianwen-1 landing site, Geophys. Res. Lett. 50 (13) (2023) e2022GL102207.

[18] V. Ciarletti, et al., Astrobiology 17 (6–7) (2017) 565–584.

[19] G.G. Ori, F. Flamini, K. Taj Eddine, Mars analogue activities: the Ibn Battuta centre and the sahara desert, European Planetary Science Congress (EPSC2015–780) (2015).

[20] M.C. Raguso, M. Mastrogiuseppe, R. Seu, L. Piazzo, Super resolution and interferences suppression technique applied to SHARAD data, in: 5th IEEE International Workshop on Metrology for AeroSpace, 2018, pp. 242–246.

[21] L. Gambacorta, M.C. Raguso, M. Mastrogiuseppe, R. Seu, UWB processing applied to multifrequency radar sounders: the case of MARSIS and comparison with SHARAD, IEEE Trans. Geosci. Rem. Sens. 60 (1–14) (2022) no. 5120014.

[22] N. Oudart, V. Ciarletti, A. Le Gall, Y. Hervé, E. Brighi, Retrieval of the ground dielectric permittivity by planetary GPR accommodated on a rover: application to the estimation of the reflectors' depth by the WISDOM/ExoMars radar, Planet. Space Sci. 224 (2022) 105606.

[23] I. Ibrar, X. Bin, T. Gang, L. Yuguo, Y. Yang, Analysis of subsurface velocity using CMP gathers picked up by unshielded GPR system: results from an experimental NAPL contaminated test site, Explor. Geophys. 54 (Issue 3) (2023) 261–270.

[24] D.E. Stillman, E. Pettinelli, S.E. Lauro, E. Mattei, G. Caprarelli, B. Cosciotti, K. M. Primm, R. Orosei, Partially-saturated brines within basal ice or sediments can explain the bright basal reflections in the South Polar layered deposits, J. Geophys. Res.: PlanetsVolume 127 (Issue 10) (2022) e2022JE007398.

[25] G.S. Baker, T.E. Jordan, J. Pardy, An introduction to ground penetrating radar (GPR), Special Paper of the Geological Society of America 432 (2007) 1–18, https://doi.org/10.1130/2007.2432(01. In book: Special Paper 432: Stratigraphic Analyses Using GPR.

[26] G. Bitella, R. Rossi, A. Loperte, A. Satriani, V. Lapenna, M. Perniola, M. Amato, Geophysical techniques for plant, soil, and root research related to sustainability, in: Book: the Sustainability of Agro-Food and Natural Resource Systems in the Mediterranean Basin. Chapter: Geophysical Techniques for Plant, Soil, and Root Research Related to Sustainability Publisher, springer open, Springer Cham Heidelberg New York Dordrecht LondonEditors, 2015, https://doi.org/10.1007/978-3-319-16357-4_23.

[27] K. Meyer, ErdogmusE, E. Erdogmus, G. Morcous, M. Naughtin, Use of ground penetrating radar for accurate concrete thickness measurements. Conference: Architectural Engineering Conference (AEI) 2008, 2008, https://doi.org/10.1061/41002(328)67.

[28] J. Gross, J. Filiberto, Granitic compositions in gabbroic martian meteorite NWA 6963 and a possible connection to felsic compositions on the martian surface. 45th Lunar and Planetary Science Conference, #1440, 2024.

[29] V. Payré, M.R. Salvatore, C.S. Edwards, An evolved early crust exposed on mars revealed through spectroscopy, Geophysical Research Letter 49 (2022) e2022GL099639.

[30] J.W. Wray, S.T. Hansen, J. Dufek, G.A. Swayze, S.L. Murchie, F.P. Seelos, J. R. Skok, R.P. Irwin, M.S. Ghiorso, Infrared spectral identification of unusually feldspar-rich rocks on Mars, in: 44th Lunar and Planetary Science Conference, #3065, 2013.

[31] F. Rivera-Hernández, D.Y. Sumner, N. Mangold, S.G. Banham, K.S. Edgett, C. M. Fedo, S. Gupta, S. Gwizd, E. Heydari, S. Maurice, N. Nachon, H. Newsom, J. Schieber, K. Stack-Morgan, N. Stein, R.C. Wiens, Grain size variations in the murray formation: stratigraphic evidence for changing depositional environments in Gale crater, mars, J. Geophys. Res. 125 (2020) e2019JE006230.

[32] M. Kobayashi, H. Miyamoto, B.D. Pál, T. Niihara, T. Takemura, Laboratory measurements show temperature-dependent permittivity of lunar regolith simulants, Earth Planets Space 75 (article id.8) (2023).

[33] S. Gyalay, F. Nimmo, Closing pores and cracking: a window to martian history from a seismic wave speed discontinuity in the crust. 53rd Lunar and Planetary Science Conference, #1633, 2022.

[34] N.A. Budden, Mars field geology. Biology, and Paleontology Workshop: Summary and Recommendations, LPI Contribution No. 968, 1998.

[35] S. Schennen, S. Wetterich, L. Schirrmeister, J. Tronicke, Seasonal impact on 3D GPR performance for surveying yedoma ice complex deposits, Sec. Cryospheric Sciences 10 (2022) article id. 741524.

[36] J. Guo, L. Li, J. Liu, L. Fu, X. Tang, Y. Wang, W. Yang, Y. Dou, S. Liu, Q. Lu, G. Shi, Y. Sun, Ground-penetrating radar survey of subsurface features at the margin of ice sheet, East Antarctica, J. Appl. Geophys. 206 (2022) article id. 104816.

[37] D. Healy, C. Katopodis, P. Tarrant, Application of Ground Penetrating Radar for River Ice Surveys, 14th Workshop on the Hydraulics of Ice Covered Rivers, 2007.

[38] A.A. Fraeman, W. Rapin, J. Bapst, L. Matthies, B.L. Ehlmann, B. Langlais, R. Lillis, A. Mittelholz, B. Weiss, C. Quantin-Nataf, J. Flahaut, M. Golombek, K.L. Siebach, V. Payre, A. Udry, M.G.A. Lapotre, J. Espley, R.O. Green, P. Sullivan, D. R. Thompson, K. Sneeder, Tenth International Conference on Mars, 2024, p. 3350. Contrib. No. 3007, 2024, id.

[39] Samantha Gwizd, Kathryn M. Stack, Raymond Francis, Fred Calef, Brett B. Carr, Chris Langley, Jamie Graff, Kristinsson Hanning, Thorarensen þorsteinn, Páll Vilhjálmur, Eiríkur Bernharðsson, Michael Phillips, Matthew Varnam, Nathan Hadland, Jahnavi Shah, Jeffrey Moersch, Udit Basu, Joana R.C. Voigt, Christopher W. Hamilton, Comparing rover and helicopter planetary mission architectures in a mars analog setting in Iceland, The Planetary Science Journal 5 (8) (2024) 35, 172.

[40] R. Aguilar, T. Meng, M. Christoffersen, S. Nerozzi, J. Holt, Subsurface Investigations of Debris-Covered Glaciers as Mars Analogs with Drone-Based Ground Penetrating Radar, in: Europlanet Science Congress 2024, EPSC2024-1271, 2024.

[41] A.S. McEwen, E.M. Eliason, J.W. Bergstrom, N.T. Bridges, C.J. Hansen, W. A. Delamere, J.A. Grant, V.C. Gulick, K.E. Herkenhoff, L. Keszthelyi, R.L. Kirk, M. T. Mellon, S.W. Squyres, N. Thomas, C.M. Weitz, Mars reconnaissance orbiter's high resolution imaging science experiment (HiRISE), J. Geophys. Res. 112 (E5) (2007) E002605.

[42] D.J. Daniel, Ground Penetrating Radar, Wiley, 2005, https://doi.org/10.1002/0471654507.eme152.

[43] Colin M. Dundas, Ali M. Bramson, Lujendra Ojha, James J. Wray, Michael T. Mellon, Shane Byrne, Alfred S. McEwen, Nathaniel E. Putzig, Donna Viola, Sarah Sutton, Erin Clark, John W. Holt, Exposed subsurface ice sheets in the Martian mid-latitudes, Science 359 (6372) (2018) 199–201.

[44] Matthew Chojnacki, Lori K. Fenton, Aaron Robert Weintraub, Lauren A. Edgar, Mohini J. Jodhpurkar, Christopher S. Edwards, Ancient martian aeolian sand dune deposits recorded in the stratigraphy of valles marineris and implications for past climates, J. Geophys. Res.: Planets 125 (Issue 9) (2020) e06510 article id.

[45] Fa Wenzhe, Ejecta Properties of Zi Wei Crater as Revealed by Chang'e-3 Lunar Penetrating Radar, 2016, 47th LPSC, #1185.

[46] J.F. Mustard, C.D. Cooper, Global distribution of dissected duricrust on Mars, in: 31th Lunar and, Planetary Science abstract id.#1168, 2000.

[47] R. Grimm, E.S. Clifford S. Heggy, C. Dinwiddie, Scattering limits to depth of radar investigation: lessons from the Bishop Tuff, in: Paper Presented at Workshop on Radar Investigations of Planetary and Terrestrial Environments, #6025, 2005.

[48] E. Heggy, S.M. Clifford, R.E. Grimm, C.L. Dinwiddie, D.Y. Wyrick, B.E. Hill, Ground-penetrating radar sounding in mafic lava flows: assessing attenuation and scattering losses in Mars-analog volcanic terrains, Journal of Geopghysical Research 111 (E6) (2006) E002589.

[49] J. Spray, Geological Models for the Uppermost Martian Crust, American Geophysical Union, 2004. Spring Meeting 2004, abstract id.P33B-05.

[50] N. Putzig, SHARAD's eye view of martian dunes. 5th International Planetary Dunes Workshop #3054, 2017.

[51] R.L. Van Dam, W. Schlager, M.J. Dekkers, J.A. Huisman, Iron oxides as a cause of GPR reflections, Geophysics 67 (2) (2002) 536–545.

[52] K. Tesic, A. Baricevic, M. Serdar, N. Gucunski, Electromagnetic property selection for GPR modelling in corrosive concrete environments, Developments in the Built Environment 17 (2024) 100302.

[53] K. Wu, G.A. Rodriguez, M. Zajc, E. Jacquemin, M. Clémen, A. De Coster, S. Lambot, A new drone-borne GPR for soil moisture mapping, Remote Sensing of Environment Remote Sensing of Environment 235 (2019) 111456.

[54] R. Orosei, S.E. Lauro, E. Pettinelli, A. Cicchetti, M. Coradini, B. Cosciotti, F. Di Paolo, E. Flamini, E. Mattei, M. Pajola, F. Soldovieri, M. Cartacci, F. Cassenti, A. Frigeri, S. Giuppi, R. Martufi, A. Masdea, G. Mitri, C. Nenna, R. Noschese, M. Restano, R. Seu, Radar evidence of subglacial liquid water on Mars, Science 361 (2018) 490–493.

[55] M.A. Kreslavsky, Seasonal brine formation in shallow subsurface on mars, 53rd LPSC Contribution 2678 (2022) 2628.

[56] Mirai Kobayashi, Arihiro Kamada, Takeshi Kuroda, Hiroyuki Kurokawa, Shohei Aoki, Hiromu Nakagawa, Naoki Terada, Effects of regolith properties on the Martian subsurface water distribution using a global climate model, European Geosciences Union General Assembly (2024) 7059.

[57] S.Y. Nikiforov, M.V. Djachkova, R. Gellert, I.G. Mitrofanov, D.I. Lisov, M. L. Litvak, A.B. Sanin, A.R. Vasavada, Water and chlorine in the martian subsurface along the 27 km traverse of NASA's curiosity rover according to DAN measurements: 2. Results for distinct geological regions, J. Geophys. Res.: Planets 129 (4) (2024) e2022JE007731.
[58] N. Roth, T. Zhu, Y. Gao, Characterizing liquid water in deep martian aquifers: a seismo-electric approach, J. Geophys. Res.: Planets 129 (2024) id. e2024JE008292.
[59] D.M.H. Baker, G.A. Morgan, A. Pathare, C.M. Dundas, N.E. Putzig, SWIM Team, Subsurface Water Ice Mapping (SWIM) on Mars: Planet-wide Geomorphic Mapping of Ice-Related Landforms, 53rd LPSC, Contrib, 2022. No. 2678, id.2669.
[60] E.L. Scheller, B.L. Ehlmann, R. Hu, D.J. Adams, J.L. Yung, Long-term drying of Mars by sequestration of ocean-scale volumes of water in the crust, Science 372 (2021) 56–62.
[61] E. Heggy, P. Paillou, G. Ruffie, J.M. Malezieux, F. Costard, G. Grandjean, On water detection in the Martian subsurface using sounding radar, Icarus 154 (2001) 244–257.
[62] E. Pettinelli, P. Burghignoli, A.R. Pisani, F. Ticconi, A. Galli, G. Vannaroni, F. Bella, Electromagnetic propagation of GPR signals in martian subsurface scenarios including material losses and scattering, IEEE Trans. Geosci. Rem. Sens. 45 (2007) 1271–1281.
[63] J.-P. Bibring, Y. Langevin, J.F. Mustard, F. Poulet, R. Arvidson, A. Gendrin, B. Gondet, N. Mangold, P. Pinet, F. Forget, Team Omega, M. Berthé, C. Gomez, D. Jouglet, A. Soufflot, M. Vincendon, M. Combes, P. Drossart, T. Encrenaz, T. Fouchet, R. Merchiorri, G.C. Belluci, F. Altieri, V. Formisano, F. Capaccioni, P. Cerroni, A. Coradini, S. Fonti, O. Korablev, V. Kottsov, N. Ignatiev, V. Moroz, D. Titov, L. Zasova, D. Loiseau, P. Pinet, S. Doute, B. Schmitt, C. Sotin, E. Hauber, H. Hoffmann, R. Jaumann, U. Keller, R. Arvidson, T. Duxbury, G. Neukum, Global mineralogical and aqueous mars history derived from OMEGA/mars express data, Science 312 (2006) 400–404.
[64] S.x Czarnecki, C. Hardgrove, R.E. Arvidson, M.N. Hughes, M.E. Schmidt, T. Henley, L.M. Martinez Sierra, I. Jun, M. Litvak, I. Mitrofanov, J. Lightholder, Hydration of a clay-rich unit on mars, comparison of orbital data to rover data, J. Geophys. Res.: Planets 128 (2023) e2021JE007104.
[65] J. Carter, L. Riu, F. Poulet, J.-P. Bibring, Y. Langevin, B. Gondet, A Mars orbital catalog of aqueous alteration signatures (MOCAAS), Icarus 389 (2023) article id. 115164.
[66] K. Hiroyuki, Hydrated crust stores Mars' missing water, Science 372 (2021) 27–28.
[67] V. Ansan, E. Hauber, M. Golombek, N. Warner, J. Grant, J. Maki, R. Deen, F. Calef, C. Weitz, J. Garvin, S. Wilson, N. Williams, C. Charalambous, T. Pike, H. Lethcoe, M. Kopp, A. De Mott, S. Smrekar, B. Banerdt, R. Lorenz, InSight landing site: stratigraphy of the regolith beneath the lander and in its surroundings, and implications for formation processes. 50th Lunar and Planetary Science Conference #1310, 2019.
[68] L.M. Carter, R. Rincon, L. Berkoski, Mapping the upper subsurface of Mars using radar polarimetry, Concepts and Approaches for Mars Exploration #4285 (2012).
[69] C.J. Bierson, S. Tulaczyk, S.W. Courville, N.E. Putzig, Strong MARSIS radar reflections from the base of martian South Polar cap may Be due to conductive ice or minerals, Geophys. Res. Lett. 48 (2021) GL093880.
[70] S.E. Lauro, E. Pettinelli, G. Caprarelli, et al., Using MARSIS signal attenuation to assess the presence of South Polar Layered Deposit subglacial brines, Nat. Commun. 13 (2022) 5686, https://doi.org/10.1038/s41467-022-33389-4.
[71] A.M. Bramson, J.L. Molaro, E.I. Petersen, Z.M. Bain, N.E. Putzig, G.A. Morgan, I. B. Smith, H.G. Sizemore, D.M.H. Baker, M.R. Perry, M. Mastrogiuseppe, R. H. Hoover, B.A. Campbel, A.V. Pathare, Polar is in the eye of the beholder: ice-rich units across the mid-latitudes of Mars. Seventh Mars Polar Science Conf. #6015, 2020.
[72] J.J. Plaut, J.W. Holt, J.W. Head, Y. Gim, P. Choudhary, D.M. Baker, A. Kress, the SHARAD Team, Thick ice deposits in Deuteronilus Mensae, Mars: regional distribution from radar sounding. 41st Lunar and Planetary Science Conference #2454, 2010.
[73] G.P. Tsoflias, M.W. Becker, Ground-penetrating-radar response to fracture-fluid salinity: why lower frequencies are favorable for resolving salinity changes, Geophysics 73 (2008), https://doi.org/10.1190/1.2957893.
[74] C. Mätzler, Microwave properties of ice and snow, in: B. Schmitt, C. De Bergh, M. Festou (Eds.), Solar System Ices, Kluwer Academic Publishers, Dordrecht, The Netherlands, 1998, pp. 241–257, 1998.
[75] R. Orosei, C. Ding, W. Fa, A. Giannopoulos, A. Hérique, W. Kofman, S.E. Lauro, C. Li, E. Pettinelli, Y. Su, S. Xing, Y. Xu, The global search for liquid water on mars from orbit: current and future perspectives. The global search for liquid water on mars from orbit: current and future perspectives, Life 10 (8) (2020) 120.
[76] J.B. Garvin, F.T. Ulaby, W. Webster, Dielectric properties of meteorites: implications for radar observations of Phobos, Lunar and Planetary Science Conference 19 (1988) 377.
[77] J.H. Bradford, J.T. Harper, J. Brown, Complex dielectric permittivity measurements from ground-penetrating radar data to estimate snow liquid water content in the pendular regime, Water Resour. Res. 45 (8) (2009) WR007341.
[78] H. Looyenga, Dielectric constants of heterogeneous mixture, Physica 31 (3) (1965) 401–406.
[79] K. Roth, R. Schulin, H. Fluhler, W. Attinger, Calibration of time domain reflectometry for water content measurement using a composite dielectric approach, Water Resour. Res. 26 (1990) 2267–2273.
[80] Koyan P, Tronicke J. 3D modeling of ground-penetrating radar data across a realistic sedimentary model. Comput. Geosci. 137, 104422.
[81] F. Tosti, C. Patriarca, E. Slob, A. Benedetto, S. Lambot, Clay content evaluation in soils through GPR signal processing, J. Appl. Geophys. 97 (2013) 69–80.
[82] F. Simas, E.C.G.R. Schaefer, V.F. Melo, M.B.B. Guerra, M. Saunders, J. GilkesR, Clay-sized minerals in permafrost-affected soils (cryosols) from king george island, Antarctica, Clay Clay Miner. 54 (6) (2006) 721–736, https://doi.org/10.1346/CCMN.2006.0540607.
[83] A. Lundberg, H. Thunehed, Snow wetness influence on impulse radar snow surveys theoretical and laboratory study, Nord. Hydrol 31 (2) (2000) 89–106.
[84] M.E. Brookfield, Aeolian processes and features in cool climates, Geological Society London Special Publications 354 (1) (2011) 241–258, https://doi.org/10.1144/SP354.16.
[85] E. Mattei, S.E. Lauro, G. Vannaroni, B. Cosciotti, F. Bella, E. Pettinelli, Dielectric measurements and radar attenuation estimation of ice/basalt sand mixtures as martian Polar Caps analogues, Icarus 229 (2014) 428–433.
[86] W.E. Medeiros, J. Oliveira, F. Santana, F. Bezerra, C. Cazarin, Enhancing stratigraphic and structural features in GPR images of limestone karst through adequate data processing, in: Near Surface Geoscience Conference & Exhibition, 2018 id. Mo-24P1-15.
[87] G. Valerio, A. Galli, P.M. Barone, S.E. Lauro, E. Mattei, E. Pettinelli, GPR detectability of rocks in a Martian-like shallow subsoil: a numerical approach, Planet. Space Sci. 62 (2012) 31–40.
[88] L. Keszthelyi, S. Self, T. Thordarson, Flood lavas on Earth, io and mars, J. Geol. Soc. 163 (2006) 253–264.
[89] R.R. Ghent, S.W. Anderson, T.M. Pithawala, The formation of small cones in Isidis Planitia, Mars through mobilization of pyroclastic surge deposits, Icarus 217 (2012) 169–183.
[90] C. Souness, B. Hubbard, R.E. Milliken, D. Quincey, An inventory and population-scale analysis of martian glacier-like forms, Icarus 217 (2012) 243–255, https://doi.org/10.1016/j.icarus.2011.10.020.
[91] S. Brough, B. Hubbard, A. Hubbard, Area and volume of mid-latitude glacier-like forms on Mars, Earth Planet Sci. Lett. 507 (2019) 10–20.
[92] M. Willmes, D. Reiss, H. Hiesinger, M. Zanetti, Surface age of the ice-dust mantle deposit in Malea Planum, Mars, Planet. Space Sci. 60 (2012) 199–206.
[93] M.G. Kleinhans, H.E. van de Kasteele, E. Hauber, Palaeoflow reconstruction from fan delta morphology on Mars, Earth Planet Sci. Lett. 294 (2010) 378–392.
[94] A. ElShafie, E. Heggy, Dielectric and hardness measurements of planetary analog rocks in support of in-situ subsurface sampling, Planet. Space Sci. 86 (2013) 150–154.
[95] M. Golombek, N. Williams, M. Cacan, H. Grip, A. Jasour, J. Maki, L. Crumpler, R. Sullivan, M. Lemmon, J. Bapst, M. Mischna, A. Sholes, J. Anderson, The Mars helicopter, Ingenuity mission, Tenth International Conference on Mars, LPI Contrib 3007 (2024) 3411.
[96] Alexandra A. Ahern, A. Deanne Rogers, Christopher S. Edwards, Sylvain Piqueux, Thermophysical properties and surface heterogeneity of landing sites on mars from overlapping thermal emission imaging system (THEMIS) observations, J. Geophys. Res.: Planets 126 (6) (2021) article id. e06713.
[97] Robin L. Fergason, Philip R. Christensen, Hugh H. Kieffer, High-resolution thermal inertia derived from the thermal emission imaging system (THEMIS): thermal model and applications, J. Geophys. Res. 111 (E12) (2006). CiteID E12004.
[98] B.S. Kumar, S. Baraha, A.K. Sahoo, S. Maiti, Enhancing subsurface exploration: a comprehensive review of advanced clutter removal techniques for ground penetrating radar imaging, Measurement 239 (2025) 115432.
[99] A. Petrosyan, B. Galperin, S.E. Larsen, S.R. Lewis, A. Määttänen, P.L. Read, N. Renno, L.P.H.T. Rogberg, H. Savijärvi, T. Siili, A. Spiga, A. Toigo, L. Vázquez, The Martian atmospheric boundary layer, Rev. Geophys. 49 (3) (2011) RG000351.
[100] Tiago P. Nascimento, Martin Saska, Position and attitude control of multi-rotor aerial vehicles: a survey, Annu. Rev. Control 48 (2019) 129–146.
[101] K. Lochan, B.K. Roy, B. Subudhi, A review on two-link flexible manipulators, Annu. Rev. Control 42 (2016) 346–367.
[102] Khamseh H. Bonyan, F. Janabi-Sharifi, A. Abdessameud, Aerial manipulation - a literature survey, Robot. Autonom. Syst. 107 (2018) 221–235.
[103] C. Qiuyu Haidong, Z. Chongfa, D. Yajie, M. Yufeng, Y. Jun, Stability research of quadcopter UAV under unstable wind, in: 2021 IEEE 7th International Conference on Control Science and Systems Engineering (ICCSSE), Qingdao, China, 2021, pp. 114–118.
[104] B. Jackson, T. Brown, Estimating near-surface Martian winds using the Ingenuity helicopter's attitude, in: 55th Lunar and Planetary Science Conference #1984, 2024.
[105] N. Katsantonis, Design of a High Wind-Resistant Unmanned Aerial Vehicle (UAV), University of Twente, 2022. BSc Thesis work.
[106] D.M.H. Baker, L.M. Carter, Probing supraglacial debris on Mars 1: sources, thickness, and stratigraphy, Icarus 319 (2019) 745–769.
[107] Jonathan, et al., Mars science helicopter: compelling science enabled by an aerial platform. Planetary science and astrobiology decadal survey 2023-2032 white paper e-id. 361, Bull. Am. Astron. Soc. 53 (Issue 4) (2021) e-id. 361.